A System for Fusing Color and Near-Infrared Images in Radiance Domain

Kim C Ng
OPPO US Research Center
2479 E Bayshore Rd, Palo Alto, CA 94070
kim.ng@oppo.com

Jinglin Shen

Chiu Man Ho

Abstract

We designed and demonstrated a system that fused color and near-infrared (NIR) images in the radiance domain. The system is designed to enhance image quality captured in outdoor environments, especially in hazy weather conditions. Previous dehazing methods based on RGB-NIR fusion exist but have rarely addressed the issue of color fidelity and potential see-through effect of fusing with NIR image. The proposed system can dehaze and enhance image details while maintaining the color fidelity and protect privacy. By working in the radiance domain, the system could handle large brightness differences among the color and NIR images and achieve High Dynamic Range (HDR). We proposed two methods to correct the fusion color: linear scalings when raw images were used and color swapping with base-detail image decomposition in the presence of nonlinearity in the ISP pipeline. The system also had two clothing see-through prevention mechanisms to avoid ethical issue arising from the see-through effect of NIR image.

1. Introduction

Image Fusion is to combine the information from all sources of images into one compact form of image. The fused image contains more information than any single source image. Image fusion from different sensory modalities is even more challenging, because the images contain different information, including colors, brightness, and details. There are literatures proposing algorithms for fusing these images [21] [12].

One of the active research area is in fusing color images (RGB) with Near-Infrared images (NIR) [14][7][2]; the recent methods also include the use of Deep Learning [20][15][26]. Some would decompose the images into bases and details [20][15][27] for fusion. [8] fused RGB with NIR in various color spaces and performed psychophysical evaluation on visual preferences. In general, the aim is to increase the details of the color image from the extra information of NIR while preserving the color and brightness of the color image; simply, we want to have the similar RGB look but with more detail enhancement from NIR.

One of the most promising application of RGB-NIR fusion is image enhancement, such as denoising[30] and dehazing[13][27][6]. We also targets the image enhancement problem under hazy weather conditions. One popular RGB-NIR dataset is development in [1], but there is no raw domain dataset available to the best of our knowledge. There are also works in dehazing using a single RGB color image [4][9][29][10][28]. Also many of these dehazing methods are effective, there are still issues to be addressed before they can apply to practical use cases such as photography on smart phones. One problem is that most existing dehazing methods focus on reducing haze in the image to the maximum extend, but may have negative image quality impact, such as producing poor white balance or introducing false colors. More severely, fusing with NIR image can potentially cause see-through effects. In this work, we design a complete RGB-NIR system to address such image quality issues.

Another aim is to increase the dynamic range of the fusion image to achieve High Dynamic Range (HDR) imaging [31]. Many algorithms as quoted above are attempting to find the optimum weights to assign to RGB and NIR for combining the two together. However, the optimum weights are difficult to be found especially if one image is dark while the other is very bright, due to their differences in imaging sensors, lens, filters, as well as camera settings such as exposure time and gains. This brightness variation happens even when both RGB and NIR images are taken synchronously on the same imaging device. Objects with the same brightness and color within a captured RGB frame can turn out to have very different brightness in NIR due to their differences in reflection and scattering characteristics [16].

Many of the current image fusion methods can add details to the fusion image; however, the resulting color deviates from the original input color image's and thus the fusion image does not look natural or its color is just plain outright wrong. [24] fused RGB with multispectral images to achieve higher resolution, we specifically fuse RGB and NIR in the radiance domain to handle the wide brightness differences in RGB and NIR and consequently also achieve HDR. As far as we know, there was no previous work trying to prevent clothing see-through.

In this paper, we also use Guided Image Filter [11] to decompose RGB and NIR into bases and details so that we can manipulate them separately and decide on the amount of NIR to be added to the RGB for preventing clothing see-through. The fusion image is then again decomposed and swapped in the base of the decomposed RGB; the decomposed details of the fusion image are added back in. This helps to maintain the original RGB color and at the same time having all the details added from the NIR. In case there are haze in the scene, the last step is to detect the haze zones and adjust their pixels' saturation for dehazing.

The way how we fuse the RGB with NIR has the following characteristics:

i. Can achieve HDR in the radiance domain.

ii. Can manipulate the desired amount of details added from NIR.

iii. Can prevent see-through clothing.

iv. Can maintain the original RGB image color.

v. Can dehaze.

2. System Overview

Our framework has distinctive modules that can control image details, colors, dehazing, and clothing see-through prevention respectively. This paper describes a system methodology that can fuse RGB and NIR in the radiance domain so that the large brightness differences among the RGB and NIR images can be fused easily and HDR can be attained. It also takes advantage of the Guided Image Filter being able to decompose images into base and detail parts; afterwards, we can recombine the parts that we care for to form a new fusion image. The base-detail decomposition/combination is used for clothing see-through prevention and maintaining the original RGB color after fusing RGB and NIR. A dehazing algorithm, such as "Localized Auto White Balance" described here, can then be applied to remove the haze from the final fusion image.

3. System Modules

Fig. 1 is a framework of how we implement a RGB + NIR image fusion system. Firstly, we need to decide if HDR is the desired effect. If yes, we need to precompute the Camera Response Function (CRF) of RGB and NIR. One notable algorithm for deriving the CRF is published by [3]. The CRFs are for converting the images to radiance domain for fusion and back to the image domain after fusion. Details of radiance domain fusion pipeline is shown

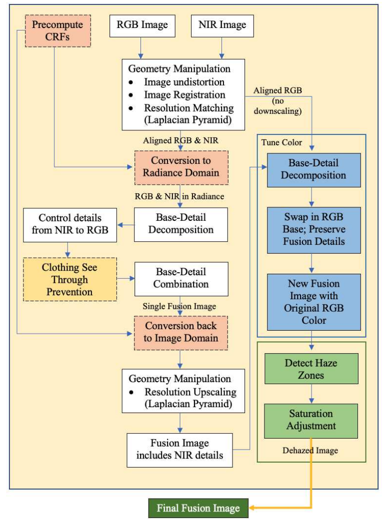

Figure 1. A system flow of RGB and NIR image fusion

in Section 3.1. If HDR is not desired, we can skip the modules of "Precompute CRFs", "Conversion to Radiance Domain", and "Conversion back to Image Domain". Note that the input images can be in the raw or any format in the ISP pipeline, although raw format is preferred.

The input RGB and NIR will go through the first module of Geometry Manipulation that the resolution of RGB and NIR need to be matched up using algorithm such as Laplacian Pyramid and aligned/registered using algorithm that can handle local adjustment [19][23]. Afterward, RGB and NIR will be converted to the radiance domain if HDR is desired, or they will be passed through as pixel values into the base-detail decomposition module using Guided Image Filter [11]. This module, described in Section 3.2, allows us to control the amount of NIR details being added to the RGB image. One possible application is to use this module to control the clothing see-through effect of the NIR (see Section 3.3). After the manipulation of NIR details, we recombine the bases and details to form a single fusion image. This image is upscaled to the higher resolution of RGB or NIR using Laplacian Pyramid. The fusion image now includes the details from the NIR.

The fusion image above, however, will have the color that deviates significantly from the original RGB's. The fusion image will next go through a post processing module to tune its color. The original RGB image is fed into the Tune Color module as a reference image. Both the original RGB image and the fusion image are decomposed into bases and details. The fusion image's base is then swapped out and replaced with the original RGB image's base. The details of the fusion image are added onto the base of the original RGB. Details can be seen in Section 3.4. This new fusion image with the original RGB color, enhanced by the NIR details, is subsequently fed into a dehazing module. The

Figure 2. Left: Original RGB image. Right: Original NIR image

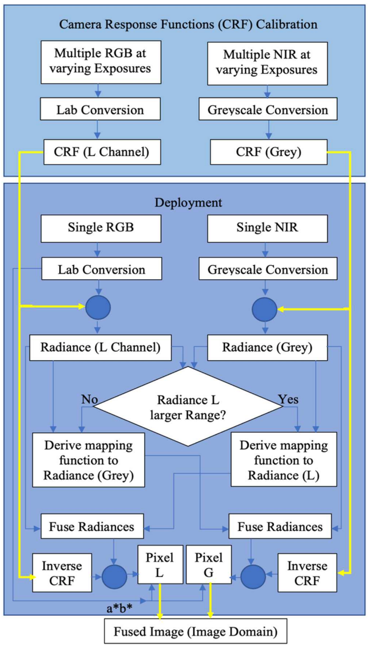

Figure 3. Fusing RGB and NIR images in the radiance domain

module will detect haze zones and adjusts their saturation accordingly to remove the white cast/haze from the image. One possible method is using our method as described in Section 3.5. Going through the entire pipeline, a final fusion image is produced with enhanced NIR details with original RGB color and dehazed.

3.1. Color Image and Near-Infrared Image Fusion in Radiance Domain

In Fig. 2, although the pixel values of the RGB and NIR are different, the radiance value of a pixel of the same object point in the scene should be the same. So, when we can transform those pixel values back to their respective radiance values, we can then combine them straightforwardly by simply averaging their values. To recover the radiance maps of RGB and NIR, we use the method published by [3]. Since we just want to extract the details of NIR and use those details to enhance the RGB, we convert the NIR image into a grayscale image and fuse with the luminance channel of the RGB (L of Lab color space). Afterward, the luminance is combined with the color channels of RGB (ab of Lab color space).

Fig. 3 shows the algorithmic flow and how the Camera Response Functions (CRF) are used for converting the images from image domain to radiance domain and then back to the image domain after fusion. CRF of RGB and NIR can be pre-calibrated with multiple RGBs and NIRs taken at various exposure times. The range of the radiance for calibration must be as large as our deployment range. Once the CRFs are obtained, we can use them during the deployment stage for fusing every captured RGB and NIR pair. Furthermore, we will need to derive a mapping function to establish the relationship of the RGB's and NIR's radiances, due to the fact that the radiances are in the relative scale and they are from two different modalities. Note that if the CRFs were pre-calibrated with a known radiance of the luminaire, we can skip deriving the mapping function. The radiance of either RGB or NIR with the lesser range will be mapped into the range of the greater. Afterwards, both radiances can be combined with a function as simple as averaging the two. After fusing the radiances, the fused radiance values can be transformed back to the image domain with the inverse of the CRF (of L or Grey, depending on which path it takes). The color channels a* and b* are then used for re-merging with the greyscale pixel of either L or G path back to a color fusion image.

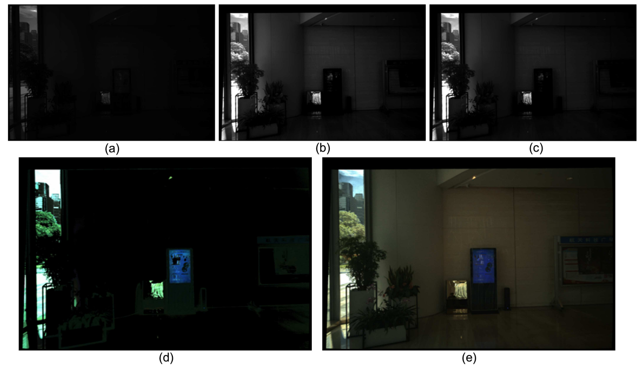

Figure 4. (a) RGB's radiance; (b) NIR's radiance; (c) NIR's radiance mapped to the range of (a); (d) Fusion image of (a) and (b); (e) Fusion image of (a) and (c).

Fig. 4 shows the radiances of RGB and NIR. RGB's radiance range is higher; the NIR's radiance must be mapped to the RGB's. Without properly mapping the RGB and NIR radiance values, when we fuse the two together, we will see the bad fusion as in Fig. 4 (d) as opposed to the properly fused image Fig. 4(e) .

Define RGB and NIR images as I_c and I_{NIR}, the fusion weights at a pixel location (x, y) can be expressed as a function of the image patches N around that pixel

$$w(x,y) = f(I_c(i,j), I_{NIR}(i,j)), i,j \in N, \qquad (1)$$

where f is a generic weight assigning function. If CRF is not available and the fusion needs to be performed in the image domain, we adopt an adaptive fusion rule developed in

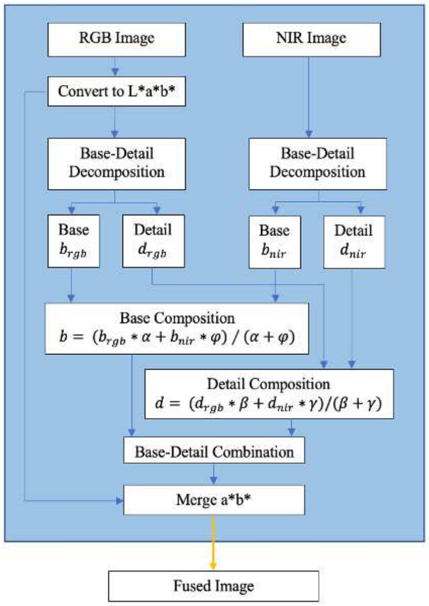

Figure 5. Fusing RGB and NIR images with base-detail decomposition and color & details adjustments

[5] that assigns fusion weights for different pixel locations to overcome the brightness differences of NIR responses, especially for vegetation regions.

3.2. Base-Detail Decomposition and Combination

Fig. 5 is the flowchart of the algorithm for decomposing the RGB and NIR images into their respective base and detail parts. First, the RGB input image is converted to a color space that we can extract its luminance channel; one such space is $L * a * b*$. If the NIR is already a monochrome image, we can just feed the image directly into the module. Guided Image Filter [11] is used for the decomposition. The bases of RGB and NIR can be composed together with the scale factors of ϕ and α. The scale factors control how much of the pixel values are weighted towards the RGB's and NIR's; this will affect the color appearance. Similarly, the details of RGB and NIR can be composed together with the scale factors of β and γ; this will affect the edge enhancement. Finally, the composed bases and details can be recombined to form a new color fusion image.

3.3. Clothing See-Through Prevention

Due to the physical characteristics of the NIR wavelength (650nm 1100nm), some material opaque to human eyes may appear transparent in NIR wavelength. This see-through effect when used for photography applications will cause privacy concerns. To the best of our knowledge, there has been very limited work addressing the clothing see-through issue in RGB-NIR fusion. It is difficult to detect and eliminate such issue using image processing methods,

Figure 6. Top row: full size NIR images captured with a man standing at different distances (1 meter, 3 meters and 10 meters). Bottom row: zoom-ins of the see-through area.

because the severity of see-through effect is correlated to the object material rather than the color or intensity information in the image domain. We have two different methods to prevent the clothing see-through issue: one is using the derived depth from the input images; second is using human detection coupled with Poisson Blending [25].

3.3.1 Depth-based

We observe that the see-through problem is mostly visible in close-up shots and the severity decreases as objects move farther away from the camera. Thus, we propose a depth-based RGB-NIR fusion method that can prevent the clothing see-through effect. Fig. 6 shows the severity of clothing see-through decreases as the distance of a standing man increases. The text under the T-shirt is clearly visible in the closeup shot at 1 meter, but it becomes less obvious as the distance increases. The text becomes barely detectable at around 10 meters.

Based on the observation of such relation between see-through capability and distance, we propose a scene depth based fusion method that will prevent close range objects from having see-through problem. We use scene depth map as a parameter in the weight assigning function during fusion, equation (1) becomes

$$w(x,y) = f(I_c(i,j), I_{NIR}(i,j), D(i,j)), i,j \in N. \quad (2)$$

where $D(i,j)$ is the estimated scene depth value in a neighborhood N of (x,y). Note that the scene depth D can be the true distance of objects from the camera, or it can be the disparity map of the scene, which is equivalent of knowing the absolute depth given the baseline of the camera system and the camera parameters. When we can recover the absolute depth of the scene, we design the weight assigning function (2) as

$$\begin{aligned} w(x,y) &= f(I_c(i,j), I_{NIR}(i,j)) * min(1, log_p(max \\ &\quad (1, \frac{D(x,y)}{D_{Cutoff}}))), i,j \in N. \end{aligned} \quad (3)$$

where D_{cutoff} is a depth threshold beyond which NIR image is not capable of seeing through objects. The value of

D_{cutoff} is dependent of the camera and lens specs, and we obtain the value from experimental results. When the system is unable to recover absolute depth, we use disparity to derive the weighting function, and the design of the weight assigning function (2) is given by

$$w(x,y) \quad = f(I_c(i,j), I_{NIR}(i,j)) * (1 - (\frac{min(D(x,y), D_{cutoff})}{D_{Cutoff}})^p), i,j \in N. \tag{4}$$

where D_{cutoff} is an experimented minimum disparity below which the see-through problem is not visible for a given NIR-RGB system, and p is a parameter what controls how fast the fusion strength decreases with depth. Using this fusion rule, we can avoid the see-through problem in the scene in Fig. 6. The fusion result is given in Fig. 7. The disparity map in Fig. 7 (b) is estimated using the MegaDepth algorithm [17]. Fusion weights calculated by Eq. (1) and Eq. (4) are shown in Fig. 7(c) and (d). The fusion weights on the person's body in Fig. 7(d) drops to nearly 0, effectively stops the NIR image from introducing transparency to the fused image. The fusion output in Fig. 7 (f)(h) are clear of see-through problem, while maintaining the desired fusion strength in the background regions.

3.3.2 Simultaneous See-Through Prevention and Deghosting with Poisson Blending

When fusing RGB with NIR, besides the aforementioned clothing see-through issue, there also exists the typical image misalignment ghosting issue associated with any multi-image registration which is required for fusing multiple images. There are numerous image registration or image alignment algorithms [32]. Even the best available algorithm cannot guarantee the non-existence of ghosts, particularly the close-up foreground objects are easy to exhibit ghosting issue due to large visual disparity. Ghosts can be detected and replaced with other pixel values to remove them from the scene [22]. Here we describe a method which can simultaneously remove foreground ghosts and prevent the clothing see-through issue.

Given two input images, one being RGB another being NIR, foreground objects or close-up humans are detected on the original input RGB image, from which foreground masks will be generated. Afterwards, the masks are dilated to some predefined number of pixels; the number of pixels can be defined as the largest disparity of the most forefront object between the RGB and NIR images, provided that the RGB and NIR sensors are mounted at a fixed location. The bounding boxes of the dilated masks are then used for extracting image portions from the input RGB. The extracted RGB's image portions are used for recomposing a new NIR by fusing them onto the original input NIR with Poisson Blending [25]. The original RGB and the newly recomposed NIR are thereafter used for image fusion. The resulting fusion image will be free of both ghosts and clothing see-through issue. The process is illustrated in Fig. 8.

3.4. Color Tuning

When the input images are raw format, the color correction can be as simple as using the scaling technique as in Section 3.4.1. due to the linearity. Otherwise, when dealing with non-linearity after the input images have been processed through various operations in the ISP, the method in Section 3.4.2. can be applied.

3.4.1 Color Correction using Raw Images

Fig. 9 shows that objects with strong IR emission are seen much brighter in the NIR image than in the RGB image. Objects in the scene with strong IR emission are the vegetation and the red road barriers. Thus, after fusing RGB and NIR, the fusion image's color will greatly deviate from the RGB's. A proper color correction algorithm will bring the color fusion image back to the natural look. Fig. 10 shows how the color can be corrected simply by adjusting the ratio of R' and B' for every pixel.

3.4.2 Color Correction with Color Swapping

After fusing the color and NIR images, we decompose the fusion image through a Guided Image Filter [11] into base and detail parts; similarly, we decompose the original input RGB image as well. The base of the input RGB image b_{RGB} can then be combined with the details of the fusion image d_{fusion} to form a new fusion image, which consequently maintains the same base color as the original input RGB image while having the newly added details of the fusion image.

Note that the amount or strength of desired details can be adjusted through d_{RGB} and d_{fusion}. These details amount can be controlled through the parameters of the Guided Image Filter.

3.5. Dehazing using Single Image Dehazing Method

If the color fusion image needs be corrected through the color swapping method in 3.4.2., some of the white haze would be added back into the fusion image. Consequently, further dehazing would be necessary. There are many available single image dehazing methods can be applied [4][9][10][28]. Here we describe a new single image dehazing method.

3.5.1 Localized Auto White Balance (AWB)

Given a RGB color image with haze, in Fig. 11, the haze zone(s) are detected. The haze zones are then passed through a Localized AWB to saturate their lower-end of the pixel values to which a specified percentage of pixels are

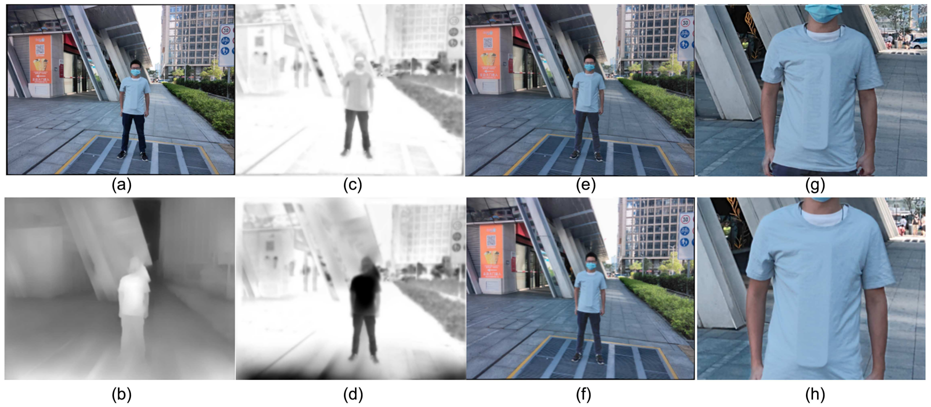

Figure 7. (a) Input image; (b) Depth image; (c) Fusion weight map without depth; (d) Fusion weight map with depth; (e)(g) Fused image using weight map (c) and the zoom-in region; (f)(h) Fused image using weight map (d) and the zoom-in region.

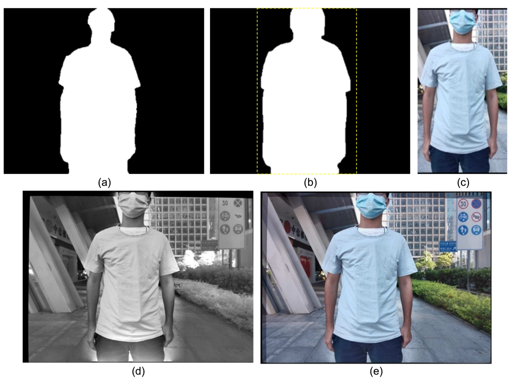

Figure 8. (a) Foreground mask derived from an imperfect depth map; (b) Dilated foreground mask; (c) Cropped RGB corresponding to yellow dashed box in (b); (d) Re-composed NIR; (e) Fused image with de-ghosting and see-through prevention.

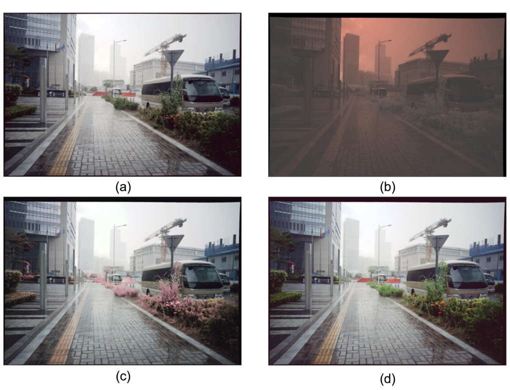

Figure 9. RGB image (a) and NIR image (b) of the same scene have different visual characteristics including color, brightness and details; (c) Fusion results of (a) (b) without color correction; (d) Fusion results of (a) (b) with color correction.

subjected. The higher the specified percentage of subjected

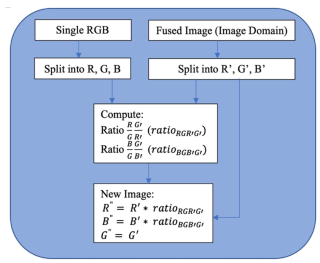

Figure 10. The flow of color correcting a fused image of raw images

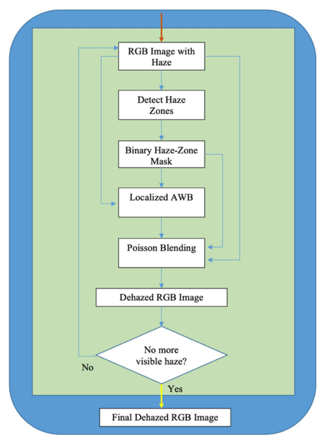

Figure 11. Flowchart of removing haze from any given hazy image

pixels, the greater the white cast or haze will be reduced. The image after the Localized AWB is Poisson blended [25] with the input RGB image to yield a dehazed image. If the image is determined still having visible haze, it can be fed back and continued to be dehazed again. Afterward, the final dehazed image is produced. One example method for detecting the haze zones can be found in [10], that can generate a transmission map; haze zones can thereafter be de-

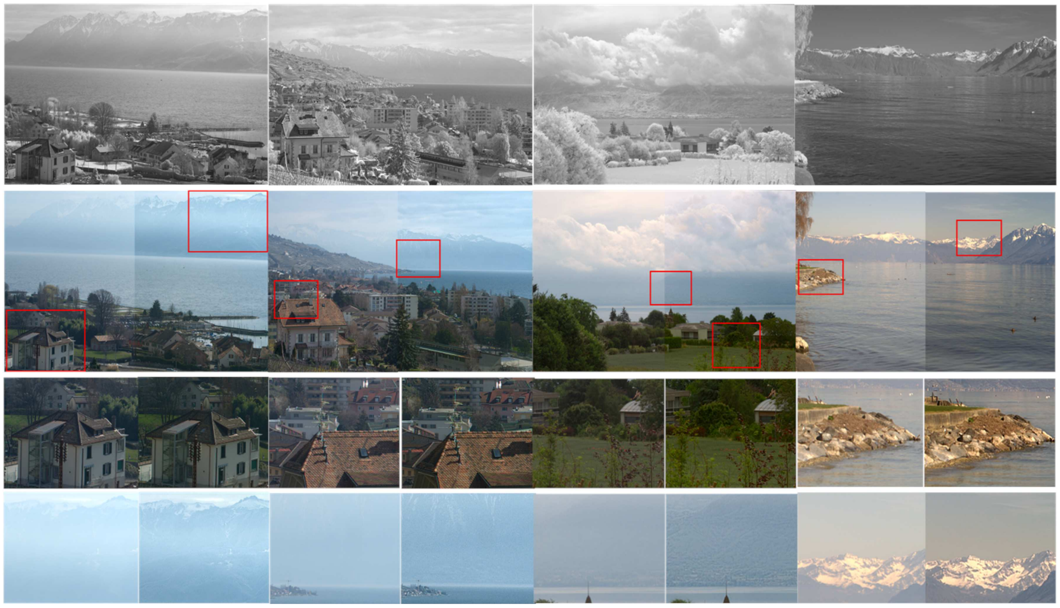

Figure 12. Fusion results on public dataset. Top row: input NIR images. Second row: Before and after fusion color images stitched side-by-side. Left half is the input image and right half is the fusion result. Third and bottom rows: Comparisons between zoomed-in regions (marked with red in the second row) of the input image and fusion output. The third row shows how well the fusion method preserves the original colors of foreground regions. The bottom row shows the dehazing capability and details enhancement in background regions.

rived from the transmission map. Our Localized AWB is modified from [18] that we only process the pixels, which are classified within the haze zones indicated by the binary haze-zone mask. Additionally, we saturate only the lower-end pixels, but leave the top-end pixels alone so that the bright pixels will not be clipped and such that the original color temperature can be preserved.

4. Experiments

We conducted experiments on both public RGB-NIR dataset from EPFL and our own dataset. For public dataset, the fusion is done in image domain instead of radiance domain because no CRF is available. Some sample results are shown in Fig. 12. As can be seen from the second row of Fig. 12, our fusion system can achieve good haze removal and detail enhancement, while preserving the color of non-hazy regions at the same time. We also compare our results to the recent de-hazing works from [13][27][6]. Note that unlike most previous dehazing algorithms whose main objective is to reduce haze to the minimum level, the goal of our fusion pipeline is to improve the overall image quality, including dehazing, detail enhancement and maintain the color accuracy after fusion. It can be seen from Fig. 13 that while achieving comparable dehazing results, our method can better maintain the original hue and color temperature. On the other hand, the results from Feng et al. and Jang et al., while effectively removes haze, significantly change the color temperature of the original image.

We further validate our entire fusion pipeline with fusion performed in the radiance domain using a dataset we collected. We built a prototype capture system based on an off-the-shelf smart phone. We replaced one of the camera modules with a 5M mono image sensor and installed a (750nm-1100nm) pass filter in front of the camera. Such system is viable for productization, because the sensor and filter we selected are both commercially available and within the cost range of comparable Bayer sensors used on nowadays smart phones. We used the main camera of the smart phone (13M) and the modified NIR camera (5M) as the capture system to capture outdoor image pairs under various weather conditions to test the proposed methods. We handle the resolution differences between the input images by decomposing the images into Laplacian pyramids and perform fusion at corresponding layers of the pyramids. Some examples are shown in Fig. 14. The different columns demonstrate the fusion results under different weather conditions. The first two columns are scenarios with heavy haze, while the input in the third and last columns have light and no haze respectively. The results show that under heavy haze conditions, the fusion pipeline can effectively remove haze, reveal details that otherwise would be invisible in RGB images, as well as keep the color unchanged in the foreground areas. For input pictures with little to no haze, the fusion results can still enhance the details of the images and increase contrast of the image, especially in sky and far away areas.

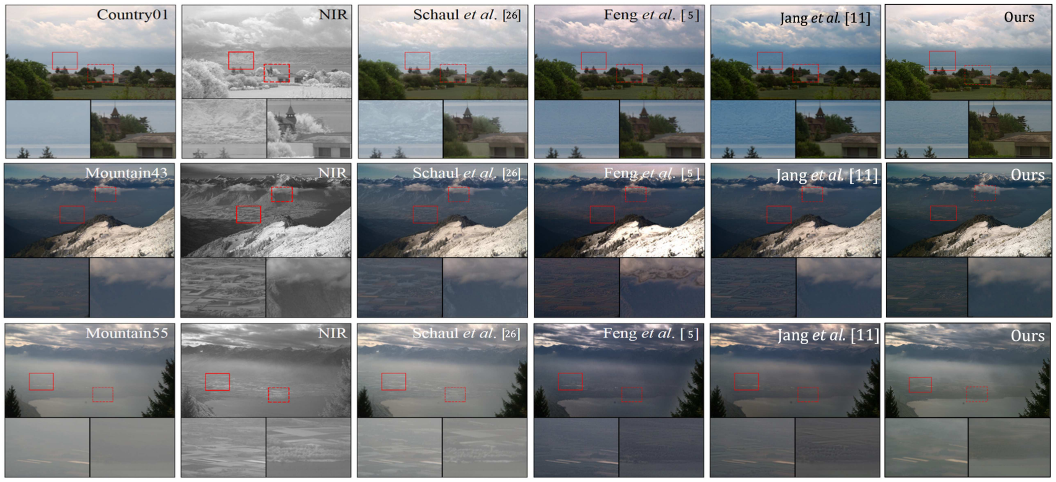

Figure 13. Comparison of our results with other dehazing methods based on RGB and NIR fusion

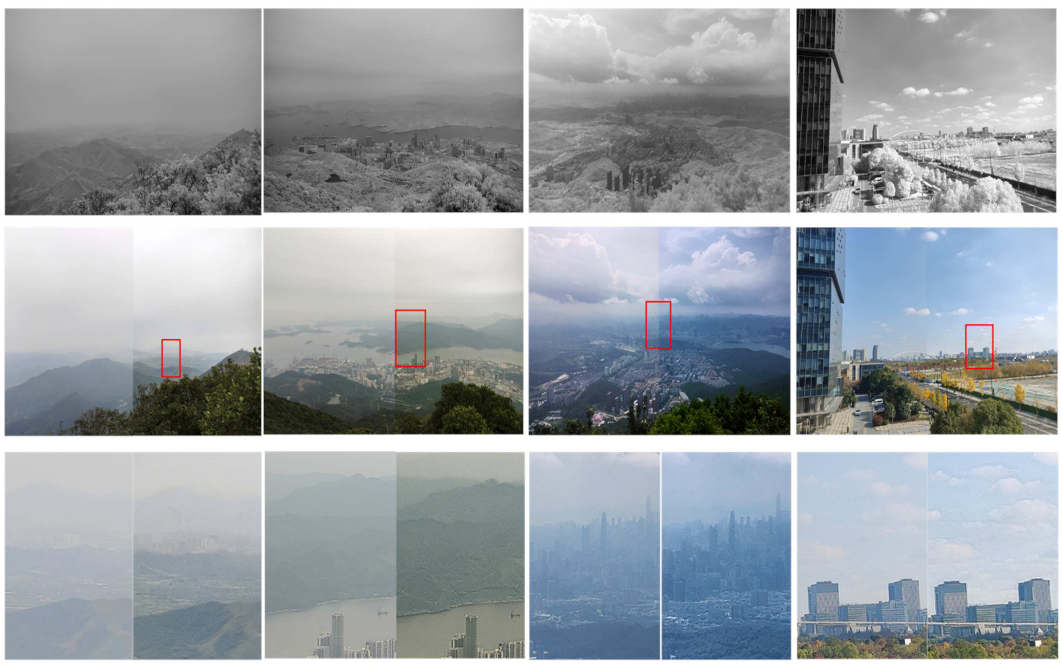

Figure 14. Fusion results on our own dataset. Top row: input NIR images. Second row: Before and after fusion color images stitched side-by-side. Left half is the input image and right half is the fusion result. Bottom rows: Comparisons between zoomed-in regions (marked with red in the second row) of the input image and fusion output.

5. Conclusion

We have developed a system which can fuse the RGB with NIR with the following characteristics:

i. Can achieve HDR in the radiance domain.

ii. Can manipulate the desired amount of details added from NIR.

iii. Can prevent see-through clothing.

iv. Can maintain the original RGB image color.

v. Can dehaze.

Our framework has distinctive modules that can control image details, colors, dehazing, and clothing see-through prevention respectively.

References

[1] Matthew Brown and Sabine Süsstrunk. Multi-spectral sift for scene category recognition. In *CVPR 2011*, pages 177–184, 2011.

[2] David Connah, Mark Samuel Drew, and Graham David Finlayson. Spectral edge image fusion: Theory and applications. In David Fleet, Tomas Pajdla, Bernt Schiele, and Tinne Tuytelaars, editors, *Computer Vision – ECCV 2014*, pages 65–80, Cham, 2014. Springer International Publishing.

[3] Paul E. Debevec and Jitendra Malik. Recovering high dynamic range radiance maps from photographs. In *Proceedings of the 24th Annual Conference on Computer Graphics and Interactive Techniques*, SIGGRAPH '97, pages 369–378, USA, 1997. ACM Press/Addison-Wesley Publishing Co.

[4] Huang Dewei, Wang Weixing, Lu Jianqiang, and Chen Kexin. Fast single image haze removal method based on atmospheric scattering model. *IFAC-PapersOnLine*, 51(17):211–216, 2018. 6th IFAC Conference on Bio-Robotics BIOROBOTICS 2018.

[5] Frederike Dümbgen, Majed El Helou, Natalija Gucevska, and Sabine Süsstrunk. Near-infrared fusion for photorealistic image dehazing. *IS&T Electronic Imaging: Proceedings*, pages 321–1–321–5(5), 2018. First two authors have equal contribution.

[6] Chen Feng, Shaojie Zhuo, Xiaopeng Zhang, Liang Shen, and Sabine Süsstrunk. Near-infrared guided color image dehazing. In *2013 IEEE International Conference on Image Processing*, pages 2363–2367, 2013.

[7] Graham D. Finlayson and Alex E. Hayes. Pop image fusion – derivative domain image fusion without reintegration. In *2015 IEEE International Conference on Computer Vision (ICCV)*, pages 334–342, 2015.

[8] Clément Fredembach and Sabine Süsstrunk. Colouring the near infrared. *Final Program and Proceedings - IS and T/SID Color Imaging Conference*, 01 2008.

[9] Zhenfei Gu, Mingye Ju, and Deng-yin Zhang. A single image dehazing method using average saturation prior. *Mathematical Problems in Engineering*, 2017:1–17, 03 2017.

[10] Kaiming He, Jian Sun, and Xiaoou Tang. Single image haze removal using dark channel prior. *IEEE Trans. Pattern Anal. Mach. Intell.*, 33:2341–2353, 01 2011.

[11] Kaiming He, Jian Sun, and Xiaoou Tang. Guided image filtering. *IEEE Transactions on Pattern Analysis and Machine Intelligence*, 35(6):1397–1409, 2013.

[12] Alex Pappachen James and Belur V. Dasarathy. Medical image fusion: A survey of the state of the art. *Information Fusion*, 19:4–19, 2014. Special Issue on Information Fusion in Medical Image Computing and Systems.

[13] Dong-Won Jang and Rae-Hong Park. Colour image dehazing using near infrared fusion. *IET Image Processing*, 11, 04 2017.

[14] Jaelin Lee, Younghyeon Park, and Byeungwoo Jeon. Low intensity rgb texture enhancement based on near infrared image using perceptual information. In *2018 10th International Conference on Communications, Circuits and Systems (ICCCAS)*, pages 422–425, 2018.

[15] Hui Li, Xiao-Jun Wu, and Josef Kittler. Infrared and visible image fusion using a deep learning framework. In *IEEE 24th International Conference on Pattern Recognition (ICPR)*, Beijing, China, 04 2018.

[16] Zhuo Li, Hai-Miao Hu, Wei Zhang, Shiliang Pu, and Bo Li. Spectrum characteristics preserved visible and near-infrared image fusion algorithm. *IEEE Transactions on Multimedia*, 23:306–319, 2021.

[17] Z. Li and N. Snavely. Megadepth: Learning single-view depth prediction from internet photos. In *2018 IEEE/CVF Conference on Computer Vision and Pattern Recognition (CVPR)*, pages 2041–2050, Los Alamitos, CA, USA, jun 2018. IEEE Computer Society.

[18] Nicolas Limare, Jose-Luis Lisani, Jean-Michel Morel, Ana Belén Petro, and Catalina Sbert. Simplest Color Balance. *Image Processing On Line*, 1:297–315, 2011.

[19] Feng Liu, Michael Gleicher, Hailin Jin, and Aseem Agarwala. Content-preserving warps for 3d video stabilization. *ACM Trans. Graph.*, 28(3), July 2009.

[20] Yaochen Liu, Lili Dong, Yuanyuan Ji, and Wenhai Xu. Infrared and visible image fusion through details preservation. *Sensors*, 19:4556, 10 2019.

[21] Jiayi Ma, Yong Ma, and Chang Li. Infrared and visible image fusion methods and applications: A survey. *Information Fusion*, 45:153–178, 2019.

[22] Kim Chai Ng. Ghost artifact detection and removal in hdr image processing using multi-level median threshold bitmaps. US Patent US9123141B2, 2013.

[23] Kim Chai Ng, Jinglin Shen, and Chiu Man Ho. Image alignment with selective local refinement resolution. US Patent Pending, 2021.

[24] Zhi-Wei Pan and Hui-Liang Shen. Multispectral image super-resolution via rgb image fusion and radiometric calibration. *IEEE Transactions on Image Processing*, 28(4):1783–1797, 2019.

[25] Patrick Pérez, Michel Gangnet, and Andrew Blake. Poisson image editing. *ACM Trans. Graph.*, 22(3):313–318, July 2003.

[26] Jingchun Piao, Yunfan Chen, and Hyunchul Shin. A new deep learning based multi-spectral image fusion method. *Entropy*, 21(6), 2019.

[27] Lex Schaul, Clément Fredembach, and Sabine Süsstrunk. Color image dehazing using the near-infrared. In *2009 16th IEEE International Conference on Image Processing (ICIP)*, pages 1629–1632, 2009.

[28] S. Shwartz, E. Namer, and Y.Y. Schechner. Blind haze separation. In *2006 IEEE Computer Society Conference on Computer Vision and Pattern Recognition (CVPR'06)*, volume 2, pages 1984–1991, 2006.

[29] Ketan Tang, Jianchao Yang, and Jue Wang. Investigating haze-relevant features in a learning framework for image dehazing. In *CVPR '14 Proceedings of the 2014 IEEE Conference on Computer Vision and Pattern Recognition*, pages 2995–3002, 2014.

[30] J. Wang, Tianfan Xue, J. T. Barron, and Jiawen Chen. Stereoscopic dark flash for low-light photography. *2019 IEEE International Conference on Computational Photography (ICCP)*, pages 1–10, 2019.

[31] Xiaopeng Zhang, Terence Sim, and Xiaoping Miao. Enhancing photographs with near infra-red images. In *2008 IEEE Conference on Computer Vision and Pattern Recognition*, pages 1–8, 2008.

[32] Barbara Zitová and Jan Flusser. Image registration methods: a survey. *Image and Vision Computing*, 21(11):977–1000, 2003.